



## Optimization of HVAC system energy consumption in a building using artificial neural network and multi-objective genetic algorithm

Nasruddin<sup>a,b,\*</sup>, Sholahudin<sup>c</sup>, Pujo Satrio<sup>a</sup>, Teuku Meurah Indra Mahlia<sup>d,e</sup>, Niccolo Giannetti<sup>f</sup>, Kiyoshi Saito<sup>c</sup>

<sup>a</sup> Department of Mechanical Engineering, University of Indonesia, Depok 16424, Indonesia

<sup>b</sup> Tropical Renewable Energy Center (TREC), Faculty of Engineering, Universitas Indonesia, Depok 16424, Indonesia

<sup>c</sup> Department of Applied Mechanics and Aerospace Engineering, Waseda University, 3-4-1 Okubo, Shinjuku-ku, Tokyo 169-8555, Japan

<sup>d</sup> School of Information, Systems and Modelling, Faculty of Engineering and Information Technology, University of Technology Sydney, NSW 2007, Australia

<sup>e</sup> Department of Mechanical Engineering, Universiti Tenaga Nasional, Selangor 43000, Malaysia

<sup>f</sup> Waseda Institute for Advanced Study, Waseda University, 1-6-1 Nishiwaseda, Shinjuku-ku, Tokyo 169-8050, Japan

### ARTICLE INFO

#### Keywords:

Radiant cooling  
Building optimization  
Neural network  
Genetic algorithm

### ABSTRACT

The optimization of heating, ventilating and air conditioning (HVAC) system operations and other building parameters intended to minimize annual energy consumption and maximize the thermal comfort is presented in this paper. The combination of artificial neural network (ANN) and multi-objective genetic algorithm (MOGA) is applied to optimize the two-chiller system operation in a building. The HVAC system installed in the building integrates radiant cooling system, variable air volume (VAV) chiller system, and dedicated outdoor air system (DOAS). Several parameters including thermostat setting, passive solar design, and chiller operation control are considered as decision variables. Subsequently, the percentage of people dissatisfied (PPD) and annual building energy consumption is chosen as objective functions. Multi-objective optimization is employed to optimize the system with two objective functions. As the result, ANN performed a good correlation between decision variables and the objective function. Moreover, MOGA successfully provides several alternative possible design variables to achieve optimum system in terms of thermal comfort and annual energy consumption. In conclusion, the optimization that considers two objectives shows the best result regarding thermal comfort and energy consumption compared to base case design.

### Introduction

The increased population growth rate has led to a greater demand for energy [1]. In 2013, the International Energy Agency (IEA) estimated that building has become the third largest energy consumer in the world [2]. Generally, energy usage in the building is expended on lighting, electrical equipment and HVAC systems. Several studies show that half of energy usage in the building is utilized for indoor climate conditioning [3,4]. Since the last decades, most of power generation systems in the world use fossil energy such as coal, oil, and natural gas as their main energy sources [5]. This does not only have the detrimental effect of generating and releasing harmful gases such as CO<sub>2</sub> and SO<sub>x</sub> into the environment, but it also further depletes the limited supply of fossil fuels. Therefore, the reduction of energy usage in buildings could minimize greenhouse gas emission. The increase in building energy consumption is highly affected by building design, change of

occupant comfort standard, building operation, maintenance, and HVAC system design. All those aspects should be conceived with energy consumption and occupant comfort in mind.

The radiant cooling system is one of the solutions that can be applied in the building to reduce the energy demand for the HVAC systems. In recent years, many researchers have paid more attention to radiant cooling technology [6]. Radiant cooling is believed to have higher energy efficiency than the conventional HVAC system in providing thermal comfort [7,8]. The reason for this is because water has a higher thermal capacity than air and a pump is generally more efficient than a fan [9]. Moreover, the temperature difference between water supply and room ambience can be very small [10]. Research on radiant cooling development has been carried out in tropical regions [11,12], and has been successfully implemented in North America and Europe [13,14]. However, it is still a new technology in tropical countries such as Indonesia and required to be developed for the application. Since this

\* Corresponding author at: Department of Mechanical Engineering, University of Indonesia, Depok 16424, Indonesia.

E-mail address: [nasruddin@eng.ui.ac.id](mailto:nasruddin@eng.ui.ac.id) (Nasruddin).

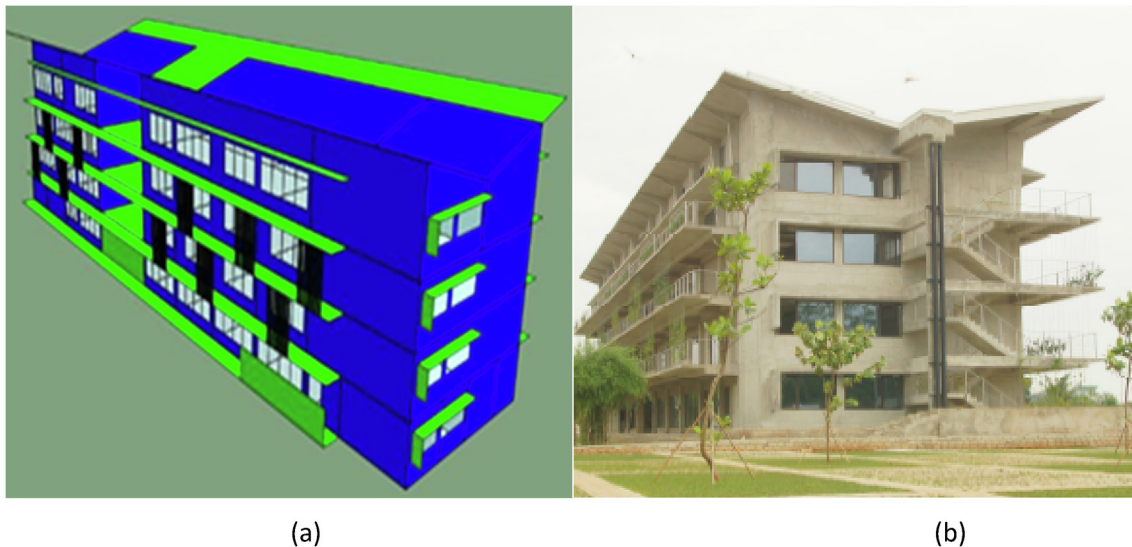


Fig. 1. Geometry of educational building (a) simulation (b) real [23].

technology is very effective in dealing with the sensible cooling load, it could work effectively in buildings with extensive use of glass, where the penetration of solar radiation into the building is very high. The main function of the radiant cooling system for tropical application is to absorb the heat emanating from the solar radiation.

In the real application, it is quite hard to determine the optimal building design and HVAC system operation in relation to environmental indoor air quality and energy consumption due to a large number of parameters that should be considered [15]. The building optimization study to improve the efficiency of HVAC system operation in the building have been conducted and published in the literature. Wang et al. [16] have developed a simplified model for the optimization and control of a cooling coil unit. Henze et al. [17] demonstrated a building model in TRNSYS with model predictive control (MPC) for thermal storage inventory at the active and passive building. Wei et al. [18] introduced particle swarm optimization (PSO) method to solve the multi objective-optimization problem of the HVAC system in a typical office facility. Freire et al. [19] used a predictive control algorithm for minimizing building energy consumption while maintaining comfortable indoor air quality. That paper presented the data-driven models to build up the relationship between input and output using the machine learning tool. The machine learning tool has been familiar and widely used in building energy research [20,21]. Kusiak et al. [20] developed ANN to build the dynamic models of the energy consumption and thermal comfort at the single HVAC system. Ferreira et al. [21] proposed radial basis neural network for predictive control to minimize HVAC energy which uses variable refrigerant flow (VRF) system. Zhou et al. [22] applied genetic algorithms to optimize building HVAC operation by minimizing energy consumption and maintaining indoor thermal comfort.

The optimization of the building HVAC system has been conducted through various methods and purpose described in the literature above. However, most of them focused on a single HVAC system that includes either radiant or VAV system only. The optimization of the combined HVAC system, including radiant cooling and VAV chiller systems operation is presented in this paper. The objective of this research is to develop a novel approach for multi-criteria optimization of building energy consumption through a MOGA optimization method, ANN, and IESVE programs. This paper addresses the multi-objective optimization of a two-chiller system where VAV and radiant system are working simultaneously, showing the potentiality of this method in determining the appropriate operation of complex HVAC systems.

## Methodology

### Thermal comfort

Thermal comfort in the building is difficult to measure since it is very subjective and highly dependent on temperature, humidity, occupant's activity, air velocity, clothing insulation, radiant temperature, and metabolic rates. Generally, every person will experience the sensation of air condition a bit differently based on their own personal habits and psychology. Two common indicators can be used to measure thermal comfort i.e. predicted mean vote (PMV) and the predicted percentage of dissatisfied (PPD) which is founded by Fanger [24]. PMV refers to the thermal scale ranging from  $-3$  (very cold) to  $+3$  (very hot). The indoor air condition can be considered to be comfortable if PMV is close to zero. PPD represents the prediction of the percentage of occupants that feel uncomfortable or dissatisfied with the air condition. Whenever PMV moves closer to zero, PPD decreases and vice versa. PPD values range from 0% to 100%.

### Building descriptions

The educational building located in West Java, Indonesia has been selected for modeling thermal comfort and energy performance. The building has a conditioned space of  $2.088 \text{ m}^2$ , a ceiling height of  $3.2 \text{ m}$ , the wall thickness of  $0.2 \text{ m}$ , and glazing areas of  $10.8 \text{ m}^2$  distributed along the south and the north wall. The building has 4-storeys and all zones are used for lecture activity. Every window is equipped with an overhang to reduce solar heat gain. The geometry of the building is presented in Fig. 1. The building construction and materials are shown in Table 1.

### HVAC systems

The building used in the present study features two chillers which are intended to supply chilled water for radiant cooling and the VAV systems. Additionally, the building is equipped with a heater to prevent condensation. The layout of the cooling system can be seen in Fig. 2. Chiller 1 with a cooling capacity of 32 TR is used for radiant cooling and chiller 2 has a cooling capacity of 41 TR for the VAV system. The radiant and VAV cooling systems work simultaneously for the building HVAC operation. The radiant systems are installed in the floor and ceiling of the building which is mostly used to handle the sensible load. On the other hand, the VAV system equipped with DOAS is utilized to

**Table 1**  
Material of building.

Layer	Wall	Roof	Floor	Window
Layer 1	Face Brick	Insulation	Soil	Solar 6MM
Layer 2	Insulation	Metal Deck	Cavity	Cavity
Layer 3	Heavy Concrete		Cavity Insulation	Clear Float 6MM
Layer 4			Metal Deck	
Layer 5			Concrete	
			Lightweight Carpet and Pad	
U-Value (W/m <sup>2</sup> .k)	0,536	0,273	0,294	2,086

*Building simulation*

Annual building energy consumption and PPD are calculated using IESVE software. Simulation is conducted by modeling the building as precisely as possible with the actual building structure presented in Fig. 1. Weather conditions are obtained from Metronome software library. The weather parameters were measured throughout ten years and the average of each parameter is used as input simulation. The input parameters for simulation including temperature, humidity, and building internal load are adopted from the actual building operation. The number of occupants varies from 2 to 12 m<sup>2</sup>/person according to the room function. Lighting and electrical equipment loads are set as 6 W/m<sup>2</sup> and 12 W/m<sup>2</sup> respectively. The cooling load generated by the occupants is set as 115 W/person where 70 W is sensible load and 45 W is latent load. The simulation is ran from 08.00 to 17.00 on weekdays and assumed that there is no activity in the building at the weekend.

The validation result of the simulation is shown in Fig. 4. The large simulation error depicted at 6:00, 15:00, 17:00, and 22:00 is highly affected by the number of occupant fluctuation which is difficult to determine exactly. However, the result of simulation shows a similar trend in chiller energy consumption compared to the real case. The validation has averaged absolute error of 63.65 kW with the chiller energy consumption ranging from 601 kW to 903 kW.

*ANN modeling*

ANN is a machine learning tool that can be used to learn the relationship between input and output variables to predict system performance. It can work like a black box model that requires no detailed parameters of the system. ANN’s working principle is inspired by the human brain as it consists of inputs, neuron, hidden layers, and output. In its simplest form, the input is multiplied by weight functions. Then the product and bias function is summed and sent into transfer functions to produce the final output. Several architectural ANN models have been successfully applied in building and air conditioning system application for predicting absorption system performance [25]; liquid desiccant system performance [26]; building heating load [27]; indoor air temperature and humidity [28].

An ANN model with multilayer perceptron network (MLP) is developed to predict annual building energy consumption and PPD values. As shown in Fig. 5, the MLP network consists of input layer, hidden layer and output layer where all inputs are connected to the neurons, and all neurons are connected to the output.

The correlation between the input  $u(k)$  and output  $y(k)$  in the MLP network can be written mathematically as follows

$$y(k) = f_2(w^2x(k) + b_2) \tag{1}$$

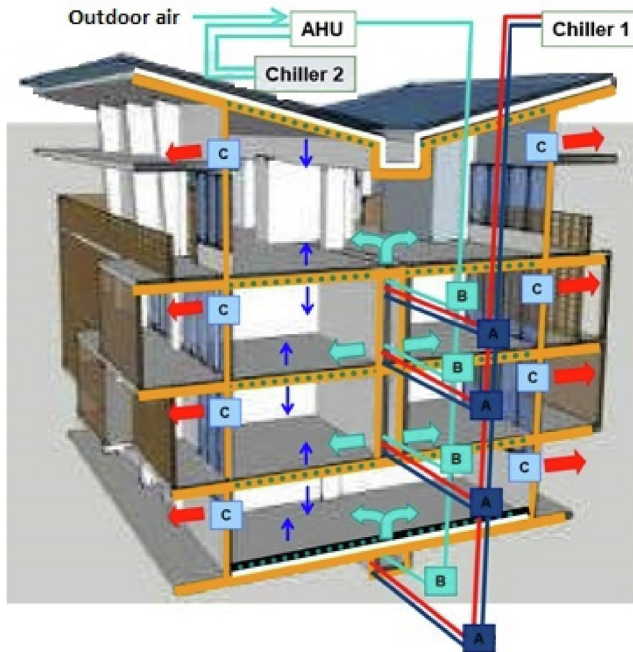


Fig. 2. HVAC system configurations [23].

deal with the latent load. The fresh air is circulated through the air handling unit (AHU) and exit via the exhaust. The schematic diagram of the radiant and VAV system is shown in Fig. 3. Chilled water flow and temperature of the radiant system is controlled manually. Meanwhile, the VAV system is controlled automatically in accordance with the cooling load.

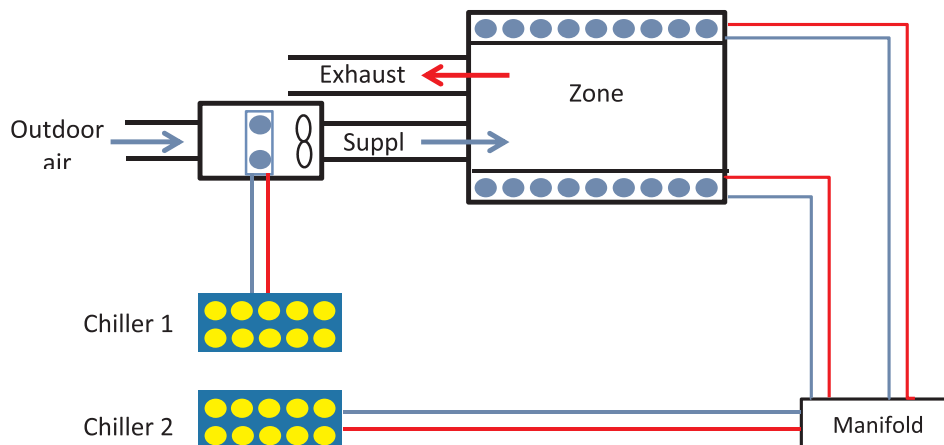


Fig. 3. Schematic diagram of radiant and VAV system [23].

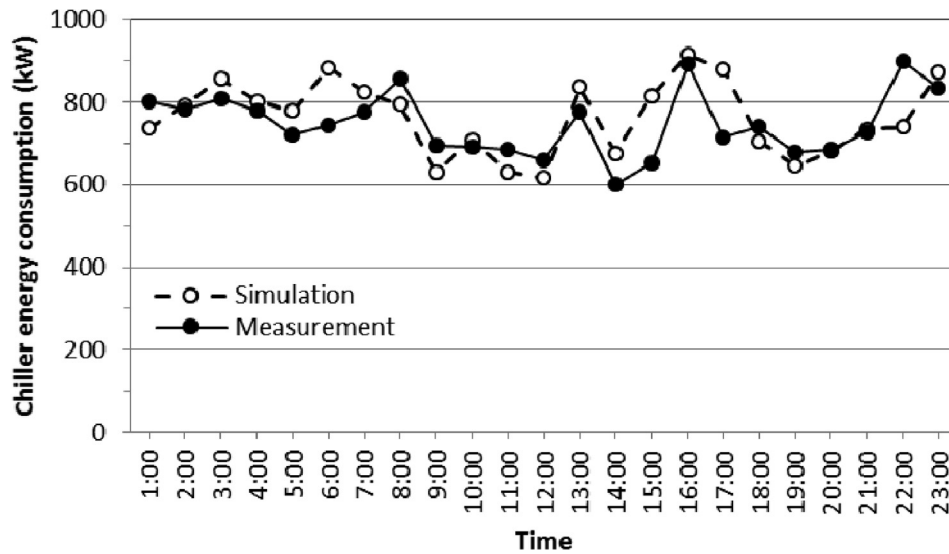


Fig. 4. Validation result of building energy simulation.

$$x(k) = f_1(w^1 u(k) + b_1) \tag{2}$$

where  $x(k)$  indicates the output vector from the hidden layer. Then  $w^2$  and  $w^1$  represent the connection weight matrix from the hidden layer to the output layer and from the input layer to the hidden layer. The notation  $b_1$  and  $b_2$  show bias numbers in the input layer and the output layer [29]. Furthermore,  $f_1(\cdot)$  and  $f_2(\cdot)$  represent the transfer functions of the hidden layer and output layer, respectively. The transfer function used in the present study is a Tangent sigmoid function that can be expressed as

$$f(z) = \frac{(1 - e^{-2z})}{(1 + e^{-2z})} \tag{3}$$

$z$  represents a function of  $z = f(\sum w_i x_i)$  where  $i$  is the index on inputs to the neuron,  $x_i$  is the input to the neuron,  $w_i$  is the weighted factor attached to the input,  $z$  is the weighted input [30]. The accuracy of prediction is measured using RMSE (root mean square error).

$$RMSE = \sqrt{\frac{1}{p} \sum_j |t_j - o_j|^2} \tag{4}$$

where  $p$  represents the number of datasets;  $t_j$  is a target;  $o_j$  is an output value respectively.

The training process is conducted by optimizing weight and bias coefficients to minimize the error between target and ANN output. The structure of ANN for the building performance prediction is shown in Fig. 6. It is designed using 10 inputs, 3 neurons, and 2 outputs. In this work, Bayesian regularization is applied to avoid overfitting and improve the generalization capability of the network.

The performance of the designed ANN configuration is evaluated by conducting training and validation using different data. The data sets

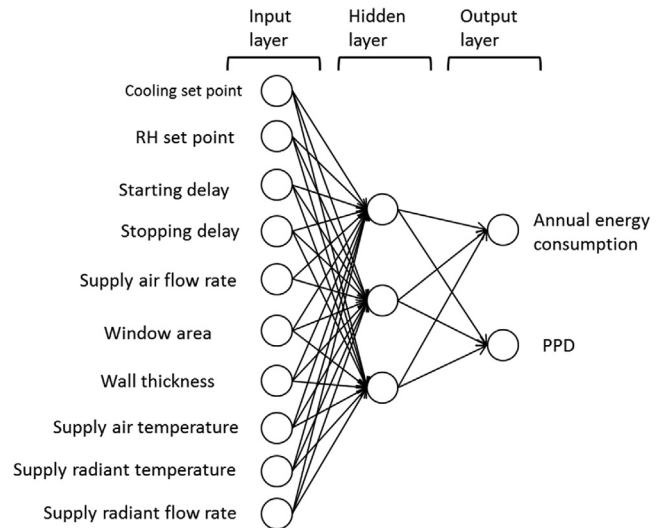


Fig. 6. The structure of ANN with inputs and outputs.

are firstly divided into two groups. The first 150 datasets are employed for training and the other 100 datasets are used for validation. The performance of training and validation is shown in Figs. 7 and 8 respectively. The training and validation result shows a strong agreement between the calculated and predicted value for both annual energy consumption and PPD. The PPD value ranges from 10.09% to 29.34%, while energy consumption ranges from 4.71 MWh to 10.81 MWh. This proves that the designed network configuration is feasible and can be

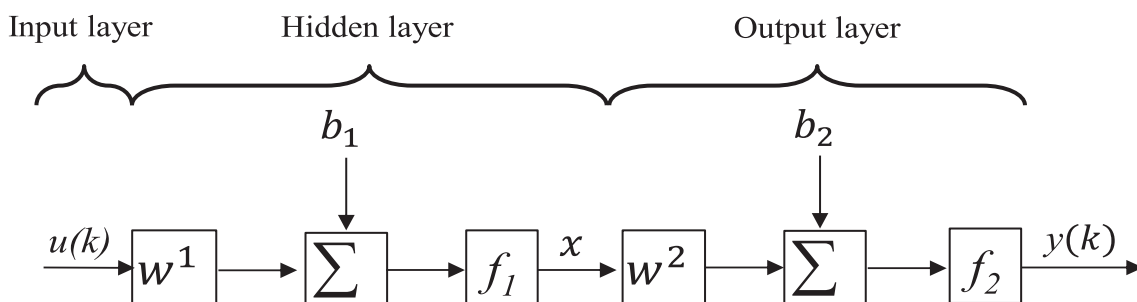


Fig. 5. Multilayer perceptron network.

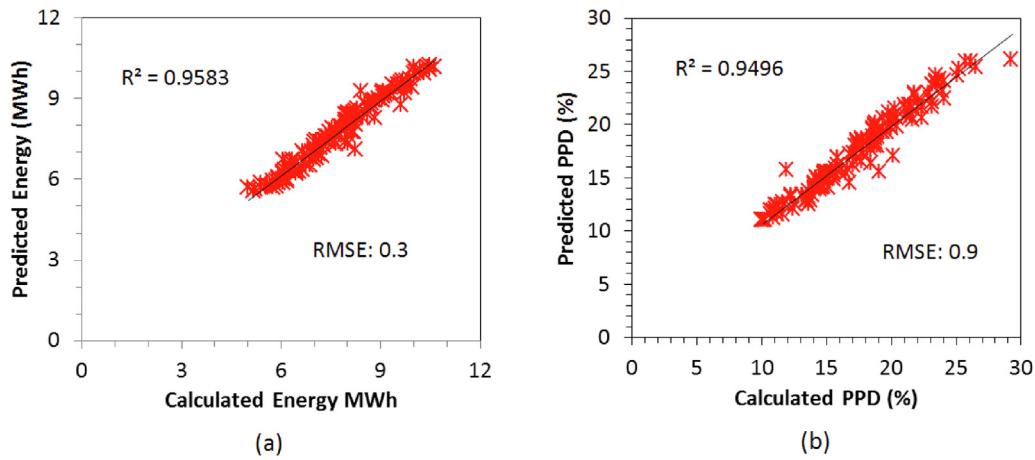


Fig. 7. Training result using 150 data sets (a) energy (b) PPD.

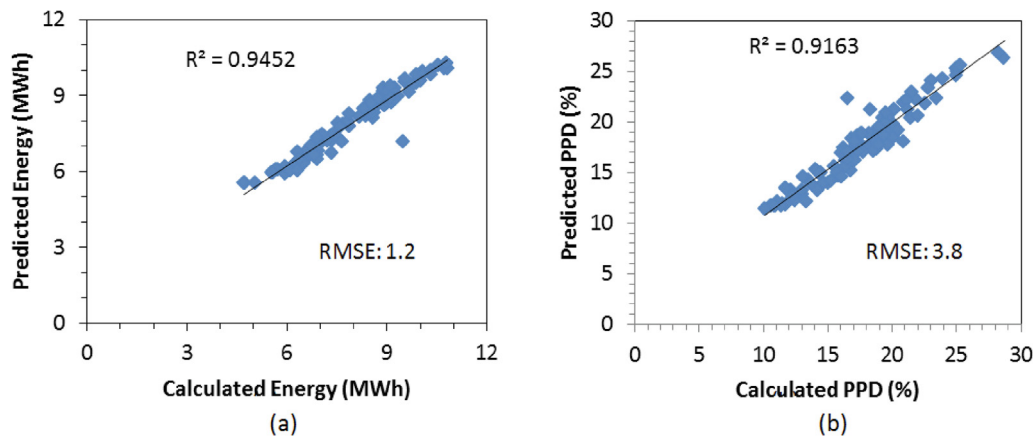


Fig. 8. Validation result using 100 data sets (a) energy (b) PPD.

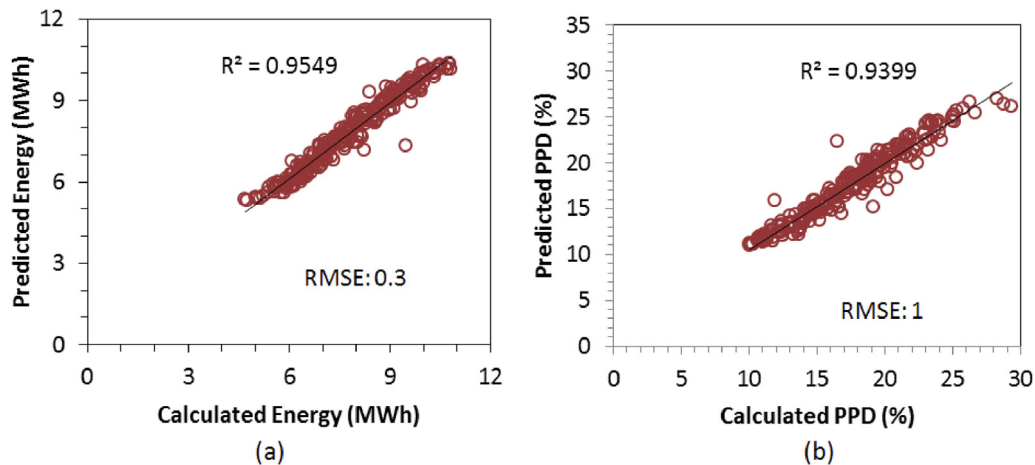


Fig. 9. Training result using 250 data (a) energy and (b) PPD.

used to predict building performance in different condition. Subsequently, all the data are included for training. The performance of training using 250 data sets is shown in Fig. 9. The result shows that the training performance using 250 and 150 data have similar degrees of accuracy, which suggests the consistency of the model to be used for prediction.

#### Optimization algorithm

Optimization algorithms are generally divided into two types, namely conventional gradient-based methods and gradient free direct methods [22]. The gradient-based method is one of the classical optimization methods which use derivatives of the objective and constraint function in searching for the optimal solution process. The performance of this algorithm is highly dependent upon the initial values supplied. It effectively converges to the optimal solution if the objective and

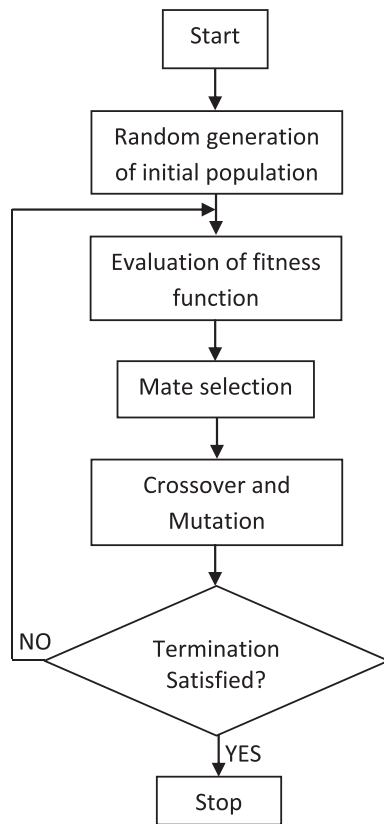


Fig. 10. Genetic algorithm processes in optimization [36].

constraint function is differentiable. Most gradient-based optimizers cannot work effectively with discontinuous or non-differentiable functions. Since the relationship of the building parameters with each other is nonlinear, which generates discontinuous function [31], this algorithm is not suitable for optimization in the building. The gradient free direct method has instead been proved to be applicable for optimization in building application [22]. This can be used to solve problems that are difficult to solve using gradient-based methods. Genetic algorithm, one of the gradient-free direct methods, has been successfully applied for optimization on HVAC system controls [32], green building design [33] and thermal and energy performances of refrigeration system [34].

Genetic algorithm work is inspired by the biological processes of reproduction and natural selection to find the fittest solution [35]. The important steps involved in this algorithm are a reproduction, selection, crossover and mutation [36]. The fundamental procedure of the genetic algorithm for the optimization process is shown in Fig. 10. It begins with population generation to produce several potential solutions to the problem. The next is conducting an evaluation on fitness function which represents the objective function that should be optimized. In this evaluation, the best parents are selected to generate the next population. After fitness evaluation, mate selection is required to allow the selected parents to undergo cross over. Furthermore, the new population is generated to replace the old one. This process works continuously until the termination criteria is met.

*Optimization approach*

Multi-objective optimization with two objective functions is employed in the present study. Annual building energy consumption and PPD are chosen to be the first and second objective functions, respectively. Several parameters obtained from the building envelope and chiller operation are selected as decision variables because they affect the annual energy consumption and PPD while the HVAC system is

**Table 2**  
Data range for optimization.

Decision variables	Range	Unit
Cooling set point	22–27	°C
Rh set point	40–60	%
Starting delay	0–30	min
Stopping delay	0–60	min
Supply air flow rate (VAV system)	140–220	L/sec
Window area	7–17	m <sup>2</sup>
Wall thickness	0.05–0.25	m
Supply air temperature (VAV system)	14–18	°C
Supply radiant temperature (radiant system)	14.8–18.5	°C
Supply radiant flow rate (radiant system)	0.2–0.4	L/sec

operating. The range of decision variables is presented in Table 2 and designed following the behavior of the actual HVAC system applied in the selected educational building. Cooling and RH set points are determined according to ASHRAE standards for tropical region application. Thermostat delays are set at different values to attain the advantage of building thermal mass to reduce energy consumption while maintaining thermal comfort. Building structural parameters, including window area and wall thickness are varied to see the effect of these variables on energy and thermal performance. Chiller supply temperature and mass flow rate are assigned to provide cooling as required.

The procedure of optimization conducted in this paper is briefly explained in Fig. 11. The process begins with the data sets fabrication by modeling and calculating annual energy consumption and PPD using IESVE software. The combination of data sets that represent 250 different conditions is produced using the Latin hypercube sampling method [37]. Every single condition is simulated within 10 min. It

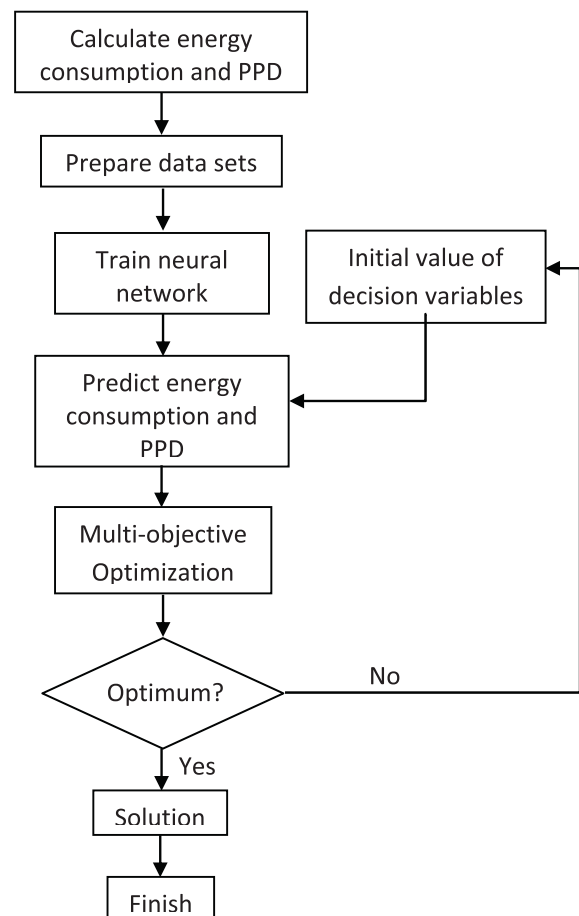


Fig. 11. Optimization framework.

required 2500 min (more than 40 h) to finish all simulations. Subsequently, the combination of ANN and MOGA is applied to solve the optimization problem. The data sets are used for training, to correlate between decision variables and two objectives using ANN. The network obtained from the above mentioned training is employed to predict PPD and building energy consumption using the new input combination which is generated by iteration of decision variables in the desired range. The minimum and maximum values of each decision variable are considered to be the lower and upper bound of optimization, respectively. Furthermore, the genetic algorithm will find the optimum solution in minimizing PPD and building energy consumption.

A multi-objective problem can be defined using the equation as follows [38]:

$$\text{Find } x = (x_i) \forall i = 1, 2, \dots, N_{par} \tag{5}$$

$$\text{Minimizing or maximizing } f_i(x) \forall i = 1, 2, \dots, N_{obj} \tag{6}$$

$$g_j(x) = 0 \quad \forall j = 1, 2, \dots, m \tag{7}$$

$$h_k(x) = 0 \quad \forall k = 1, 2, \dots, n \tag{8}$$

where  $x$  represents the decision variable vectors,  $N_{par}$  indicates number of decision variables,  $f_i(x)$  is objective function,  $N_{obj}$  is number of objective functions,  $g_j(x)$  and  $h_k(x)$  describes equality and inequality constraints, while  $m$  and  $n$  shows number of equality and inequality constraints.

## Results and discussion

### Optimization result

The optimization of the HVAC system has been accomplished using ten decision variables and two objectives. Fig. 12 shows the Pareto optimal solution for optimization of annual energy consumption and PPD in the building. It clearly indicates the conflict between the two objective functions. The decrease in energy consumption ranging from 4.76 MWh to 7.48 MWh led to a rise in PPD from 8.17% to 15%. Point A provides the solution with the minimum PPD (8.17%), which represents the maximum thermal comfort. However, this is associated with the highest energy consumption (7.48 MWh). Conversely, point B provides the solution with the lowest energy consumption (4.76 MWh), but very high in PPD (15%). Point B would have been chosen if energy was considered as the only objective. Meanwhile, point A is the best solution for a case where thermal comfort is the main priority.

In the multi-objective optimization method, all results provided in Pareto front are non-dominated [39]. They can be preferred arbitrarily as the solution according to the acceptable range of the desired criteria. Practically, one solution that represents the desired operating point

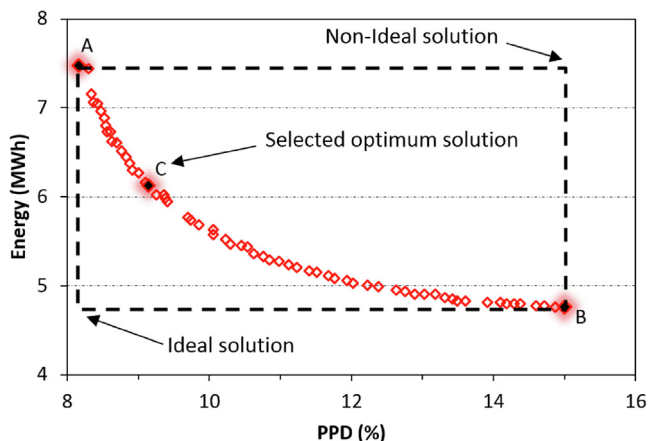


Fig. 12. Optimization result of building and HVAC system.

**Table 3**  
Optimization result of building design.

Parameters	Base case	A	B	C	Unit
Cooling set point	24.50	23.11	27	23.89	°C
RH set point	–	43.98	42.58	43.17	%
Starting delay	0.25	1.01	0.69	0.92	min
Stopping delay	0.50	1.07	1.08	0.97	min
Supply airflow rate	190.96	184.41	155.5	183.8	L/sec
Window area	10.80	7.17	7.05	7	m <sup>2</sup>
Wall thickness	0.20	0.25	0.25	0.25	m
Supply air temperature	23.00	14.35	16.59	14.3	°C
Radiant supply temperature	22.00	15.68	15.3	15.55	°C
Supply radiant flow	0.20	0.3	0.39	0.35	L/sec
PPD	27.50	8.17	15	9.14	%
Annual energy consumption	4.40	7.48	4.76	6.12	MWh

should be taken. The technique for order preference by similarity to an ideal solution (TOPSIS) is chosen to select the most optimum solution. This method has been frequently used to select the final optimum design point in similar optimization problems [40,41]. In TOPSIS decision making method, ideal and non-ideal solutions should be determined first. The ideal solution is obtained from the optimum value of each single objective, while the worst values of each objective are considered to be a non-ideal solution [39]. Consequently, the optimum solution can be assigned by selecting the point which has the shortest distance with the ideal solution and the furthest distance with the non-ideal solution [42].

In Fig. 12, the optimum solution selected while considering two objectives is indicated by point C, which is associated with energy consumption and PPD of 6.12 MWh and 9.14%, respectively. Table 3 demonstrates the corresponding value of optimal designed variables resulting from the multi-objective optimization method. Comparison of energy consumption and PPD value between the base case and the optimization result is also presented in Table 3. The base case represents the simulation condition where design variables are adopted from the existing educational building during the operation period. The base case simulation shows lower energy consumption (4.4 MWh) compared to the optimized design (point C), however, its PPD is very high (27%). According to ASHRAE standards, the acceptable PPD for thermal comfort should be less than 10% [39]. Therefore, the solution in point C can be considered to improve thermal comfort while assuring low energy consumption.

During the optimization process, most decision variables generally iterate to find the value in a wide range to reach all optimal trade-offs between two objectives. However, there are some variables set in the lower or upper bound value. The prevailing result in the optimization shows that the starting and stopping delays set to a minimum value indicating these parameters effect are not significant on the objectives. Moreover, wall thickness and window area also tend to set in the maximal and minimal values, respectively for all cases. The larger thermal mass led to a decrease in thermal resistance and an increase in heat capacity of the wall. Then a smaller window area can reduce heat gain from solar radiation. Hence the change of window area and wall thickness does not have much effect on the conflict between two objectives in the optimization problem. Furthermore, for temperature, humidity, supply temperature and mass flow both in the radiant and VAV system are essential in providing proper thermal comfort.

### Effect of cooling and RH set point

Fig. 13 shows the simulation results depicting the effect of cooling and humidity set point on energy consumption and PPD. Changing these two parameters led to variations in energy consumption and PPD. The cooling setpoint is varied from 22 °C to 27 °C and other variables are set to be constant close to an optimum value. While humidity variable range from 40% to 90%. As the temperature and humidity set

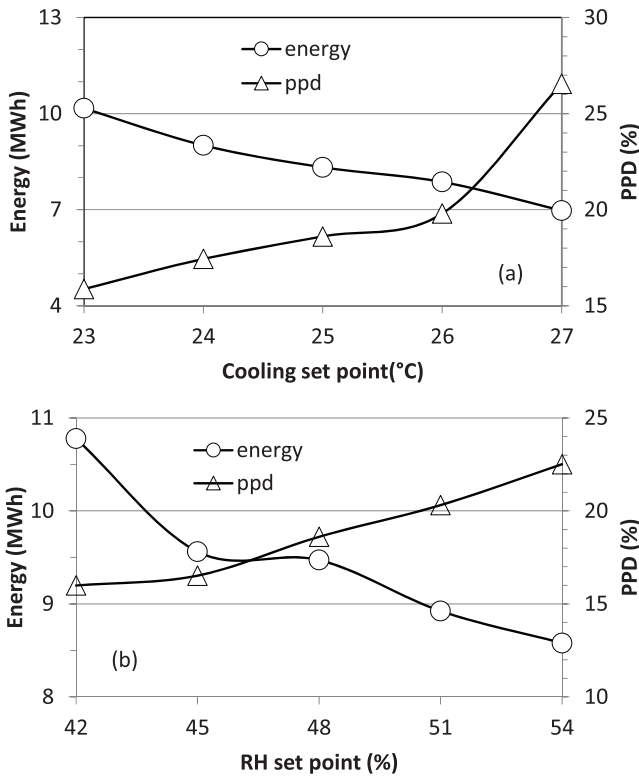


Fig. 13. Effect of (a) cooling and (b) humidity set point on annual energy consumption and PPD.

point increases, the energy required to maintain indoor air in comfortable air conditioned decreases. This is due to the fact that when the temperature and humidity difference between a set point and ambient is slight, the workload of the HVAC system, including the cooling and dehumidifier system is less. Subsequently, the increase in temperature and humidity set point causes PPD to increase. It is clear that when the temperature and humidity set point moves further from the comfort range standard, the PPD goes up.

Based on the optimization result presented in Table 3 the cooling set point at around 23 °C for point A and C conforms to the ASHRAE standard for indoor air temperature comfort. However, for point B, the cooling setpoint is set at 27 °C. Since the gap between ambient temperature and the cooling set point is small, the energy required for cooling is low. It is obvious that point B has the lowest energy consumption compared to others due to the high cooling set point. The RH setpoint is set to around 42–43%, which is still in the comfortable range [43].

Effect of supply air temperature and flow rate

Fig. 14 shows the simulation results describing the effect of supply air temperature and flow rate on annual energy consumption and PPD. The performance of the VAV system is highly affected by these two parameters. The variation of supply air flow rate and temperature causes a change in the heat removal and annual energy consumption of the VAV system. In Fig. 14(a) supply air temperature is varied from 15 °C to 23 °C with other variables set at constant values. As the supply air temperature increases, the energy from chiller required to maintain the air room condition decreases because the workload of the chiller system is depending on the temperature difference between ambient and supply air temperature. Since energy consumed by VAV chiller is dominant, consequently the higher supply air temperature leads to a lower workload of a chiller system, otherwise the lower supply air temperature will result in the higher workload of the VAV chiller

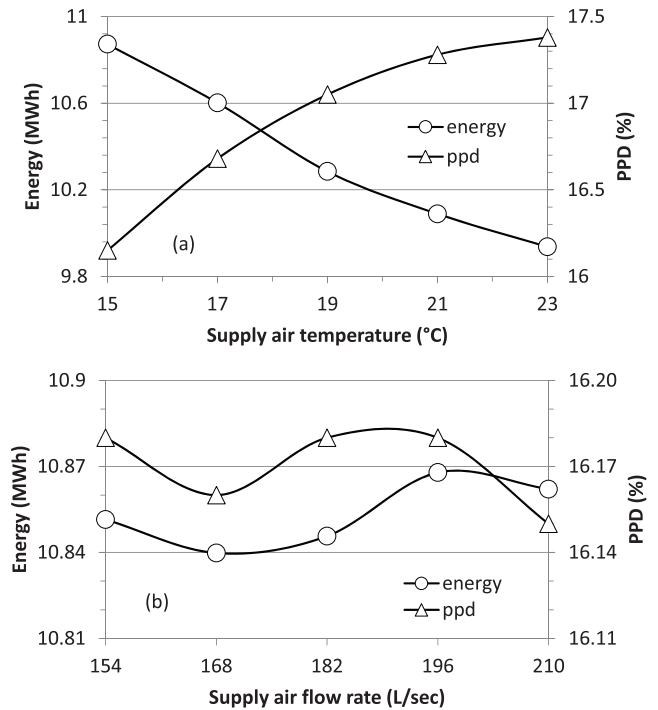


Fig. 14. Effect of supply air (a) temperature (b) flow rate on annual energy consumption and PPD.

system. Moreover, the increase in supply air temperature causes an increase of PPD owing to a slower cooling process. When the temperature difference between cooling set point and supply air temperature is moderate, it takes a longer time to achieve a room temperature within the comfort range. Hence, if the supply air temperature moves further away from the comfort range standard, PPD increases. Otherwise, when a lower supply air temperature is provided, PPD decreases.

In Fig. 14(b) supply air flow rate is varied with other parameters are set to be constant. The change in supply air flow rate leads to energy consumption and PPD fluctuate. However, Fig. 14(b) indicates that, as the supply air flow rate is ranging from 154 L/Sec to 210 L/Sec, a very small change in energy consumption and PPD is observed. In the present study, it can be noted that the energy consumed by the fan for air circulation in the VAV system is not dominant among total energy consumption of the HVAC system. Furthermore, the effect of supply air flow rate is not as significant as the supply air temperature, which it is directly related to thermal comfort.

Effect of supply radiant temperature and flow rate

Fig. 15 shows the simulation results of supply radiant temperature and the flow rate effect on annual energy consumption and PPD. In this simulation, only supply radiant temperature and the flow rate are varied and other parameters are set to be constant to demonstrate the effect of these two parameters on energy consumption and PPD. The supply radiant temperature and the flow rate are varied from 16 °C to 20 °C and 0.24 L/Sec to 0.4 L/Sec, respectively. The rise of supply radiant temperature causes higher energy consumption and PPD goes up. This can be explained considering that, when the temperature difference between supply radiant temperature and the cooling set point is small and radiant flow rate is constant, the contribution of radiant cooling system to remove the heat is less. Consequently, the VAV chiller system works very hard to cover a required cooling capacity to achieve the desired temperature. Theoretically, a higher supply radiant temperature is related to the lower energy consumption of the chiller for the radiant system. However, the change of supply radiant temperature from 16 °C to 20 °C leads to an increase in the energy consumption by

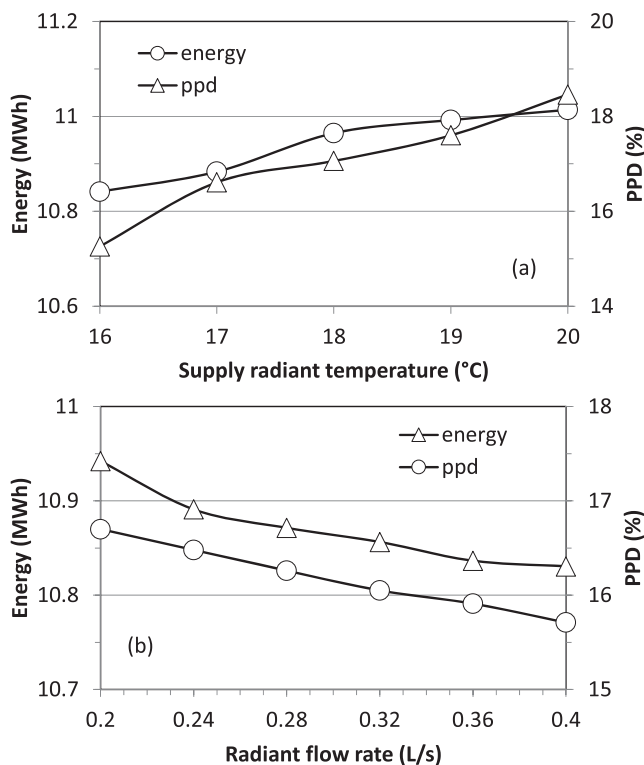


Fig. 15. effects of supply radiant (a) temperature (b) flow rate on annual energy consumption and PPD.

approximately 1.57%. This is small if we compare it with the energy consumed by the VAV chiller system, where the change of supply air temperature from 15 °C to 23 °C causes a decrease in the energy consumption around 8.6%. Hence the energy consumption of the VAV chiller system is dominant within this combined HVAC system.

Furthermore, the effect of supply radiant temperature on PPD is similar to the effect of the supply air flow temperature. If the supply radiant temperature is close to the comfort temperature the standard PPD will decrease and vice versa. In Fig. 15(b) the increase in supply radiant flow rate from 0.24 L/Sec to 0.4 L/Sec causes a decrease in energy consumption by approximately 1%. Since a higher supply radiant flow rate leads to a higher cooling capacity that can be provided to remove the heat load, when the radiant flow rate increases the workload of chiller decreases. Correspondingly, the thermal comfort can be achieved quickly. Thus, the increase of supply radiant temperature will decrease energy consumption and PPD even though in a small amount.

## Conclusions

In this work, a university building equipped with radiant cooling and VAV systems has been modeled and simulated to evaluate annual energy consumption and thermal comfort performance through PPD value. Multi-objective optimization methodology that combines ANN and MOGA has been successfully applied for defining the optimal building operation. The designed ANN configuration shows a precise prediction in the training phase with the RMSE of 0.3 and 1 for energy consumption and PPD, respectively. According to the optimization results, the multi-objective optimization shows a significant improvement in HVAC operation as for thermal comfort, while keeping low annual energy consumption when compared to the base case design. The spreading solution generated in the Pareto front provides many alternative design options. The research conducted in this paper can be used to help building management to design and select a control strategy to operate HVAC systems effectively. The research methodology applied in

the present study can be referred to solve complex optimization problems on HVAC systems and building designs.

## Acknowledgements

The authors would like to thank DRPM Universitas Indonesia for Hibah Publikasi Artikel di Jurnal Internasional Kuartil Q1 dan Q2 (Q1Q2) Tahun Anggaran 2019 Grant No. NKB-0316/UN2.R3.1/HKP.05.00/2019. We acknowledge also the support provided by PT Holcim Indonesia, Tbk and ATMI Cikarang for their permission to conduct the measurement and Ms. Sasha Media who helped us in collecting data.

## Appendix A. Supplementary data

Supplementary data to this article can be found online at <https://doi.org/10.1016/j.seta.2019.06.002>.

## References

- [1] Nasruddin, Idrus Alhamid M, Daud Y, Surachman A, Sugiyono A, Aditya HB, et al. Potential of geothermal energy for electricity generation in Indonesia: a review. *Renew Sustain Energy Rev* 2016;53:733–40.
- [2] Transition to Sustainable Buildings. Paris, France: International Energy Agency; 2013.
- [3] Poel B, van Cruchten G, Balaras CA. Energy performance assessment of existing dwellings. *Energy Build* 2007;39:393–403. <https://doi.org/10.1016/j.enbuild.2006.08.008>.
- [4] Balaras C, Dascalaki E, Gaglia A, Drousta K, Kontoyiannidis S. Energy performance of European buildings. Proceedings of the energy sustainability conference, long beach, USA. 2007. p. 387–96.
- [5] Reda AM, Ali AHH, Morsy MG, Taha IS. Design optimization of a residential scale solar driven adsorption cooling system in upper Egypt based. *Energy Build* 2016;130:843–56.
- [6] Tian Z, Love JA. Energy performance optimization of radiant slab cooling using building simulation and field measurements. *Energy Build* 2009;41:320–30.
- [7] Bourdakis E, Kazanci OB, Olesen BW. Load calculations of radiant cooling systems for sizing the plant. *Energy Proc* 2015;78:2639–44.
- [8] Memon RA, Chirattananon S, Vangtook P. Thermal comfort assessment and application of radiant cooling: a case study. *Build Environ* 2008;43:1185–96.
- [9] Park SH, Chung WJ, Yeo MS, Kim KW. Evaluation of the thermal performance of a Thermally Activated Building System (TABS) according to the thermal load in a residential building. *Energy Build* 2014;73:69–82.
- [10] Zhao K, Liu X-H, Jiang Y. Application of radiant floor cooling in a large open space building with high-intensity solar radiation. *Energy Build* 2013;66:246–57.
- [11] Nutprasert N, Chaiwiwatworakul P. Radiant cooling with dehumidified air ventilation for thermal comfort in buildings in tropical climate. *Energy Proc* 2014;52:250–9.
- [12] Simmonds P, Gaw W, Holst S, Reuss S. Using radiant cooled floors to condition large spaces and maintain comfort conditions. *ASHRAE Trans* 2000;106(1):695–701.
- [13] Hamed AM. Desorption characteristics of desiccant bed for solar dehumidification/humidification air conditioning systems. *Renew Energy* 2003;28:2099–111.
- [14] Stetiu C. Energy and peak power savings potential of radiant cooling systems in US commercial buildings. *Energy Build* 1999;30:127–38.
- [15] Magnier L, Haghighat F. Multiobjective optimization of building design using TRNSYS simulations, genetic algorithm, and artificial neural network. *Build Environ* 2010;45:739–46.
- [16] Wang Y, Cai W, Soh Y, Li S, Lu L, Xie L. A simplified modeling of cooling coils for control and optimization of HVAC system. *Energy Convers Manage* 2004;45:2915–30.
- [17] Henze GP, Kalz DE, Liu S, Felsmann C. Experimental analysis of model-based predictive optimal control for active and passive building thermal storage inventory. *HVAC & R Res* 2005;11(2):184–214.
- [18] Wei X, Kusiak A, Li M, Tang F, Zeng Y. Multi-objective optimization of the HVAC (heating ventilation, and air conditioning) system performance. *Energy* 2015;83:294–306.
- [19] Freire RZ, Oliveira GHC, Mendels N. Predictive controllers for thermal comfort optimization and energy savings. *Energy Build* 2008;40(7):1353–65.
- [20] Kusiak A, Li M-Y. Cooling output optimization of an air handling unit. *Appl Energy* 2010;87(3):901–9.
- [21] Ferreira PM, Ruano AE, Silva S, Conceicao EZE. Neural networks based predictive control for thermal comfort and energy savings in public buildings. *Energy Build* 2012;55:238–51.
- [22] Zhou L, Haghighat F. Optimization of ventilation system design and operation in office environment Part I: methodology. *Build Environ* 2009;44:651–6.
- [23] Satrio P, Sholahudin S, Nasruddin. Performance evaluation of radiant cooling system application on a university building in Indonesia. *AIP Conference Proceedings* 1826, 020018 2017. <https://doi.org/10.1063/1.4979234>.
- [24] Fanger PO. Thermal comfort. Copenhagen: Danish Technical Press; 1970.
- [25] Nasruddin, Sholahudin, Alhamid MI, Saito K. Hot water temperature prediction

- using a dynamic neural network for absorption chiller application in Indonesia. *Sustain Energy Technol Assess* 2018;30:114–20.
- [26] Mohammad AT, Mat SB, Sulaiman MY, Sopian K, Al-abidi AA. Artificial neural network analysis of liquid desiccant regenerator performance in a solar hybrid air-conditioning system. *Sustainable Energy Technol Assess* 2013;4:11–9.
- [27] Sholahudin S, Han H. Heating load predictions using the static neural networks method. *Int J Technol* 2015;6:946–53.
- [28] Mba L, Meukam P, Kemajou A. Application of artificial neural network for predicting hourly indoor air temperature and relative humidity in modern building in humid region. *Energy Build* 2016;121:32–42.
- [29] Ren Lina, Yanxin L, Zhiyuan R, Haiyan L, Ruicheng F. Application of Elman neural network and matlab to load forecasting. *International conference on information technology and computer science*. 2009. p. 55–9.
- [30] Mohanraj M, Jayaraj S, Muraleedharan C. Applications of artificial neural networks for refrigeration, air-conditioning and heat pump systems—a review. *Renew Sustain Energy Rev* 2012;16:1340–58.
- [31] Wetter M, Wright J. A comparison of deterministic and probabilistic optimization algorithms for nonsmooth simulation-based optimization. *Build Environ* 2004;39:989–99.
- [32] Huang W, Lam HN. Using genetic algorithms to optimize controller parameters for HVAC systems. *Energy Build* 1997;26(3):277–82.
- [33] Wang W, Zmeureanu R, Rivard H. Applying multi-objective genetic algorithms in green building design optimization. *Build Environ* 2005;40:1512–25.
- [34] Nasruddin, Sholahudin S, Giannetti N, Armas. Optimization of a cascade refrigeration system using refrigerant C3H8 in high temperature circuits (HTC) and a mixture of C2H6/CO2 in low temperature circuits (LTC). *Appl Therm Eng* 2016;104:96–103.
- [35] Goldberg DE. *Genetic algorithms in search, optimization, and machine learning*. Reading: Addison-Wesley; 1989.
- [36] Rajasekar N, Jacob B, Balasubramanian K, Priya K, Sangeetha K, Sudhakar Babu T. Comparative study of PEM fuel cell parameter extraction using Genetic Algorithm. *Ain Shams Eng J* 2015;6:1187–94.
- [37] McKay MD. *Sensitivity and uncertainty analysis using a statistical sample of input values, uncertainty analysis*. CRC Press; 1988. p. 145–86.
- [38] Shirazi A, Aminyavari M, Najafi B, Rinaldi F, Razaghi M. Thermal–economic–environmental analysis and multi-objective optimization of an internal-reforming solid oxide fuel cell–gas turbine hybrid system. *Int J Hydrogen Energy* 2012;37:19111–24.
- [39] Aminyavari M, Najafi B, Shirazi A, Rinaldi F. Exergetic, economic and environmental (3E) analyses, and multi-objective optimization of a CO2/NH3 cascade refrigeration system. *Appl Therm Eng* 2014;65:42–50.
- [40] Ahmadi MH, Sayyaadi H, Mohammadi AH, Barranco-Jimenez MA. Thermo-economic multi-objective optimization of solar dish-Stirling engine by implementing evolutionary algorithm. *Energy Convers Manage* 2013;73:370–80.
- [41] Abdollahi G, Sayyaadi H. Application of the multi-objective optimization and risk analysis for the sizing of a residential small-scale CCHP system. *Energy Build* 2013;60:330–44.
- [42] Yue Z. A method for group decision-making based on determining weights of decision makers using TOPSIS. *Appl Math Model* 2011;35:1926–36.
- [43] Ashrae. *ANSI/ASHRAE Standard 55-2004, Thermal environmental conditions for human occupancy*. Atlanta: American Society of Heating, Refrigerating, and Air-Conditioning Engineers, Inc.; 2004.